



Crystal nucleation and dendrite growth of metastable phases in undercooled melts

Dieter Herlach*

Institut für Materialphysik im Weltraum, Deutsches Zentrum für Luft- und Raumfahrt, D-51170 Köln, Germany

ARTICLE INFO

Article history:

Received 28 July 2010

Received in revised form

27 September 2010

Accepted 28 November 2010

Available online 3 December 2010

Keywords:

Containerless processing

Undercooling

Crystal nucleation

Dendritic growth

Supersaturated alloys

Disorder trapping

Metastable solids

ABSTRACT

An undercooled melt possesses an enhanced free enthalpy that opens up the possibility to crystallize metastable crystalline solids in competition with their stable counterparts. Crystal nucleation selects the crystallographic phase whereas the growth dynamics controls microstructure evolution. We apply containerless processing techniques such as electromagnetic and electrostatic levitation to containerless undercool and solidify metallic melts. Owing to the complete avoidance of heterogeneous nucleation on container-walls a large undercooling range becomes accessible with the extra benefit that the freely suspended drop is directly accessible for in situ observation of crystallization far away from equilibrium. Results of investigations of maximum undercoolability on pure zirconium are presented showing the limit of maximum undercoolability set by the onset of homogeneous nucleation. Rapid dendrite growth is measured as a function of undercooling by a high-speed camera and analysed within extended theories of non-equilibrium solidification. In such both supersaturated solid solutions and disordered superlattice structure of intermetallics are formed at high growth velocities. A sharp interface theory of dendrite growth is capable to describe the non-equilibrium solidification phenomena during rapid crystallization of deeply undercooled melts. Eventually, anomalous growth behaviour of Al-rich Al–Ni alloys is presented, which may be caused by forced convection.

© 2010 Elsevier B.V. All rights reserved.

1. Introduction

If a melt is cooled crystal nucleation sets in as soon as the temperature is decreased below the equilibrium temperature. This is true in most practical cases of production of materials from the liquid state. Under such circumstances the melt solidifies to the stable solid state. However, if the melt is essentially undercooled below the equilibrium melting temperature a liquid of enhanced free enthalpy is created that enables the system to choose between various solidification pathways into metastable solids. According to the well-known Ostwald's rule metastable systems nucleate to a lower-energy metastable phase rather than to the stable phase [1]. In case of deep undercoolings crystal nucleation preselects the crystallographic phase, stable or metastable. Subsequent crystal growth controls the evolution of metastable grain refined microstructures. Within nucleation theory one distinguishes between heterogeneous and homogeneous nucleation [2]. Heterogeneous nucleation is an extrinsic process in which foreign phases as container walls and metal-oxides participate in the nucleation process. The foreign phases catalyse the nucleation process by lowering the activation energy, and, therefore, limit the undercoolability of a melt. In case of

homogeneous nucleation it is assumed that any external influence on the nucleation process is avoided. Homogeneous nucleation is therefore an intrinsic process, in which the activation energy exclusively depends on the interfacial energy between solid and liquid and the difference of the Gibb's free energy of the undercooled liquid and the respective solid state. It determines the physical limit of maximum undercoolability of any material. Consequently, the complete avoidance of heterogeneous nucleation favours the solidification of metastable phases.

We apply techniques of containerless undercooling like electromagnetic levitation (EML) [3] and electrostatic levitation (ESL) [4] to undercool metallic melts. By the complete avoidance of heterogeneous nucleation on container walls and far reduction of heterogeneous nucleation on the free surface of the liquid sample by processing under high purity environment (EML) and even ultra high vacuum (ESL) conditions, a large undercooling range is achieved. At the same time, a freely suspended drop offers the extra benefit that it is directly accessible for in situ diagnostics by applying proper diagnostic means. The maximum undercoolings of pure zirconium are studied by measuring the distribution function of undercooling. For each experiment over 100 subsequent undercooling and solidification cycles are performed. The experimental data are analysed within a statistical approach of classical nucleation theory. After nucleation subsequent crystal growth completes solidification. Since we are dealing with undercooled

* Corresponding author. Tel.: +49 22036012332; fax: +49 22036012255.

E-mail address: dieter.herlach@dlr.de

melts crystal growth takes place by the growth of dendrites. The dynamics of dendrite growth is driven by the negative temperature gradient in front of the solid/liquid interface, which is due to the release of the heat of fusion during crystallization. In addition, in alloys a concentration gradient is established that drives the dendrite growth [5]. At small undercoolings growth velocity is rather sluggish and could be comparable to fluid flow velocity within the melt induced by forced convection in samples, which are electromagnetically levitated [6]. In the present work comparative experimental results are presented which were obtained by measurements of dendrite growth velocities as a function of undercooling on $\text{Al}_{50}\text{Ni}_{50}$ either in reduced gravity during parabolic flight missions and sounding rocket experiments (μg) or under terrestrial conditions (1 g). An anomalous growth velocity–undercooling relation was found by measurements under 1 g of Al-rich Al–Ni alloys such that the growth velocity decreases with increasing undercooling, behaviour not reported so far in literature. If the undercooling increases deviations from local equilibrium at the solidification front are expected. Deviation from chemical equilibrium lead to solidification of metastable supersaturated alloys described by solute trapping [7] or to the crystallization of disordered phases in intermetallics by disorder trapping [8]. Measurements of rapid dendrite growth on solid solutions and intermetallics are reported and discussed with respect to solute and disorder trapping.

2. Experimental

Samples were prepared from zirconium, aluminium and nickel all of purity of 4N5. The weight components are pre-melted in an arc furnace under high purity argon gas (6N). Pure Zr and alloys of $\text{Al}_{100-x}\text{Ni}_x$ with $x=50$ and 31.5 were prepared. The samples of zirconium were placed in the ultra-high-vacuum chambers of electromagnetic and electrostatic levitators. The temperature is measured by pyrometers with an absolute accuracy of ± 5 K. Samples in diameter of 7 mm are processed by electromagnetic levitation. The compensation of the gravitational force needs minimum power absorption to electromagnetically levitate the sample. Heat radiation is not sufficient to transfer the heat produced in the levitated sample and to cool it below its melting temperature. Therefore, forced convection by helium of high purity is used to cool the sample [3]. In the electrostatic levitator samples in diameter of 2 mm are processed under ultrahigh vacuum conditions ($\approx 10^{-8}$ mbar). Levitation and heating is decoupled in contrast to the electromagnetic levitator [4]. A high-speed video camera (Photron VKT) was applied (frame rate up to 50 000 pictures per second) to measure the radial dendrite growth velocity as a function of undercooling for Al–Ni alloys in terrestrial experiments [9]. The TEMPUS facility for containerless processing in reduced gravity [10] was used during several parabolic flight missions operated by ESA and DLR to measure the growth velocity as a function of undercooling of $\text{Al}_{50}\text{Ni}_{50}$ by the same high-speed camera as utilized for terrestrial experiments. During the sounding rocket mission TEXUS 44 EML2 the dendrite growth velocity was measured of Raney type $\text{Al}_{88.5}\text{Ni}_{31.5}$ alloy. Three undercooling and solidification cycles were obtained. The sample undercooled to $\Delta T_1 = 185$ K and $\Delta T_2 = 228$ K, respectively. The TEMPUS facility is equipped with a video camera of frequency of 200 pictures per second. During recalescence, three pictures were taken, which allow the determination of the growth velocity with an accuracy of ± 15 –25%.

3. Results and discussions

3.1. Crystal nucleation

Fig. 1 shows a temperature–time profile measured on a zirconium sample processed in the electrostatic levitator (cf. inset). First, the solid sample is heated up to its melting temperature. The sample melts congruently at the melting temperature T_m . The step in the melting plateau is due to the change of spectral emissivity when the solid transforms to the liquid. After complete melting the liquid sample is heated to a temperature well above T_m before cooling. If spontaneous nucleation sets in at an undercooling $\Delta T = T_m - T_n$ (T_n : nucleation temperature) the nucleated crystal rapidly grows. The rapid release of the heat of crystallization leads to a steep rise of temperature during recalescence. Usually, the solidification of an undercooled metallic melt is a two-staged process. During recalescence a fraction of the sample, f_R , solidifies under non-equilibrium

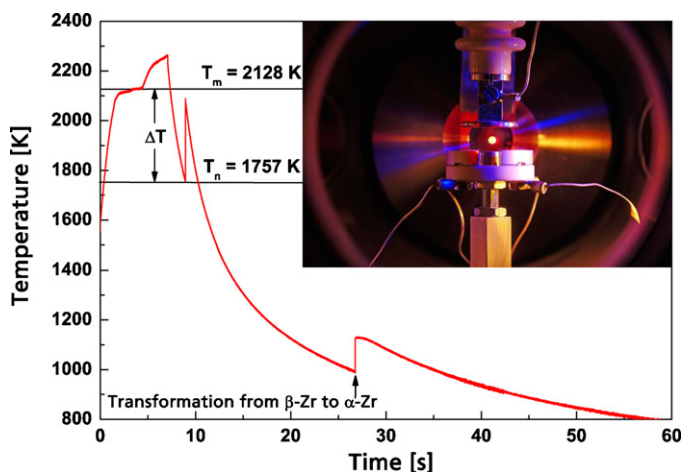


Fig. 1. Temperature–time profile recorded during melting, undercooling and solidification of pure Zr during electrostatic levitation [16].

condition. During post-recalescence the remaining melt, $f_{DR} = 1 - f_R$, solidifies under near-equilibrium condition. The fraction of the sample, f_R increases with undercooling and becomes unity, $f_R = 1$ if $\Delta T = \Delta T_{hyp}$. The hypercooling limit, ΔT_{hyp} is reached if the heat of fusion ΔH_f is just sufficient to heat the sample with its specific heat C_p up to the melting temperature. In case if the amount of heat transferred to the environment is negligible compared with the heat produced during recalescence, the hypercooling-limit is given by $\Delta T_{hyp} = \Delta H_f / C_p$. In case of pure Zr the hypercooling-limit is estimated as $\Delta T_{hyp} = 359$ K with $\Delta H_f = 14652$ J/mol and $C_p = 40.8$ J/mol/K [11]. With increasing undercooling, $\Delta T > \Delta T_{hyp}$, the melting temperature will be not reached during recalescence. As can be seen from Fig. 1 experiments on Zr using the electrostatic levitator allows for undercoolings greater than ΔT_{hyp} . This is the first time that undercoolings beyond the hypercooling limit is unambiguously observed for a pure metal, while in case of the alloy Co–Pd hypercoolings in the range of 250–300 K are reported [12]. The undercooling ΔT is easily inferred since the nucleation temperature is well defined by the onset of recalescence. For each series of measurements about 100 undercooling and solidification runs were performed.

Fig. 2 shows the distribution functions measured in the electromagnetic levitator (left) and the electrostatic levitator (right). To analyze the experimental results we refer to a model of the statis-

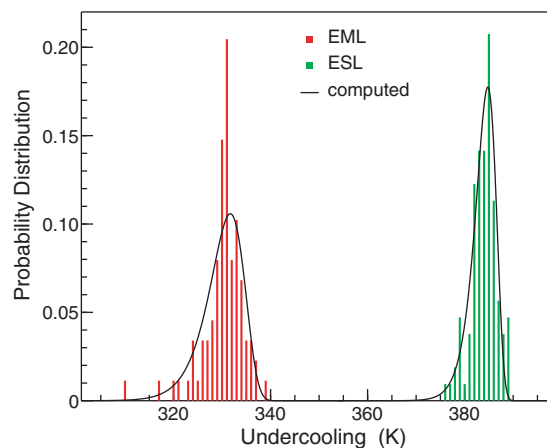


Fig. 2. Probability distribution functions of undercoolings measured in 100 experiment cycles on pure Zr in the electromagnetic (left) and the electrostatic levitator (right). The solid lines give the probability distribution function as computed according to a statistical analysis of nucleation undercooling [16].

tics of nucleation undercooling [13] and extended for application of the analysis of undercooling distribution functions [14]. It has been previously applied successfully to investigate nucleation behaviour in Co–Pd alloys with high magnetic Curie-temperatures [15]. Also the application of this model on the experimentally determined distribution function leads to interesting results on the physical nature of the nucleation processes in drops electromagnetically or electrostatically levitated [16]. In particular, a very large kinetic prefactor in the nucleation rate was found from the measurements of maximum undercooling by electrostatic levitation under the conditions of an ultra-high-vacuum environment. Such a high kinetic prefactor in the order of $K_V \approx 10^{40} \text{ m}^{-3} \text{ s}^{-1}$ is indicative for homogeneous nucleation. If homogeneous nucleation is assumed a lower limit of the dimensionless interfacial energy α to form a critical nucleus of bcc structure in Zr is estimated to be $\alpha \geq 0.61$. The comparison with modelling results shows that the negentropic model [17] with a value of $\alpha = 0.70$, gives the best agreement with the present experiment. Density-functional theory yields $\alpha = 0.46$ and $\alpha = 0.48$ [18] and molecular dynamics simulations yields $\alpha = 0.29, 0.32$, and 0.36 [19] depending on the potentials used for the simulations. All these values underestimate the solid–liquid interfacial energy inferred from the experiments. Only in the negentropic model a polytetrahedral short-range order in the interface is explicitly taken into account. Polytetrahedral short-range order in liquid metals is directly confirmed by neutron [20] and X-ray [21] diffraction on pure metallic liquids.

3.2. Influence of convection on dendrite growth

$\text{Al}_{50}\text{Ni}_{50}$ was chosen for the investigations on growth kinetics under the conditions of forced convection on Earth and reduced convection in reduced gravity [22]. This alloy melts congruently and forms an intermetallic B2 β -phase under equilibrium conditions. Crystallization of ordered superlattice structures requires short-range atomic diffusion at the solid–liquid interface. This leads to sluggish growth dynamics at least at small and intermediate undercoolings ($V: 0.1\text{--}0.5 \text{ m/s}$) [23]. These growth velocities are directly comparable to the speed of fluid flow in electromagnetically levitated metallic melts due to the strong stirring effects of the alternating electromagnetic field [6]. Fluid flow motion inside the liquid drop changes the growth dynamics. This effect, however, will be reduced if the liquid drops are processed in a reduced gravity environment since electromagnetically induced convection and natural convection are much less pronounced. Fig. 3 shows the results of measurements of dendrite growth velocity as a function of undercooling for $\text{Al}_{50}\text{Ni}_{50}$ alloy, both under terrestrial conditions (circles) and in reduced gravity (diamonds). All growth velocities measured in reduced gravity are much smaller than those determined under terrestrial conditions. At growth velocities exceeding the fluid flow velocity $V > U \approx 0.6 \text{ m/s}$ data of dendrite growth velocity from terrestrial and from reduced gravity experiments coincide. The results of sharp interface modelling neglecting the influence of fluid flow are depicted in Fig. 3 (solid line). It describes the experimental results obtained in reduced gravity. The sharp interface model was extended to take into account the influence of convection [24]. It is able to reproduce the experimental results obtained on ground if a fluid flow velocity of $U \approx 1.2 \text{ m/s}$, is assumed (cf. dashed line in Fig. 3). At growth velocities $V > 0.6 \text{ m/s}$, the computed relation of $V = f(\Delta T)$ without and with convection converge to one line since in this region the dynamics of solidification is mainly limited by thermal diffusivity.

The growth dynamics of $\text{Al}_{50}\text{Ni}_{50}$ alloy shows the usual behaviour. The dendrite growth velocity increases with increasing undercooling. This behaviour is understood by the fact that the driving force for crystallization scales with the undercooling. However, if the concentration of Al is increased to 68.5 at% Al (Raney type

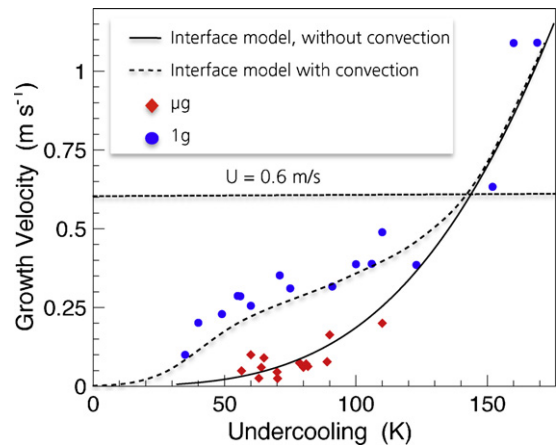


Fig. 3. Dendrite growth velocity of B2 β -phase of $\text{Al}_{50}\text{Ni}_{50}$ alloy as a function of undercooling measured under terrestrial conditions (circles) and in reduced gravity (diamonds). The solid line represents the prediction of dendrite growth theory without convection and the dashed line with convection. U denotes the speed of fluid flow inside an electromagnetically droplet as estimated by magneto-hydrodynamic simulations [6].

alloy), a monotonous decrease of the growth velocity with increasing undercooling is measured as shown in Fig. 4. In situ observation of phase selection in undercooled melts of $\text{Al}_{68.5}\text{Ni}_{31.5}$ by energy dispersive X-ray measurements at the European Synchrotron Radiation Facility Grenoble (France) unambiguously demonstrates that over the entire undercooling range $\Delta T < 320 \text{ K}$ the intermetallic B2 β -phase is primarily formed [25]. It subsequently transforms by a peritectic reaction $L + \text{AlNi} \rightarrow \text{Al}_3\text{Ni}_2$. The in situ diffraction investigations indicate that this phase is primarily formed even at highest levels of undercooling. This means that various phase reaction processes cannot explain the unusual behaviour of the growth dynamics observed for Raney alloy during the early stage of crystallization.

The Raney type alloy was studied with respect to dendrite growth dynamics during the sounding rocket mission TEXUS 44 of European Space Agency (ESA) and German Aerospace Center (DLR). The filled triangles in Fig. 4 show the growth velocity V as a function of undercooling of Raney type $\text{Al}_{68.5}\text{Ni}_{31.5}$ alloy as retrieved from the TEXUS experiment [26]. Two significant and important differences of the experiments under normal gravity and in microgravity are observed. First, the growth velocity measured in microgravity

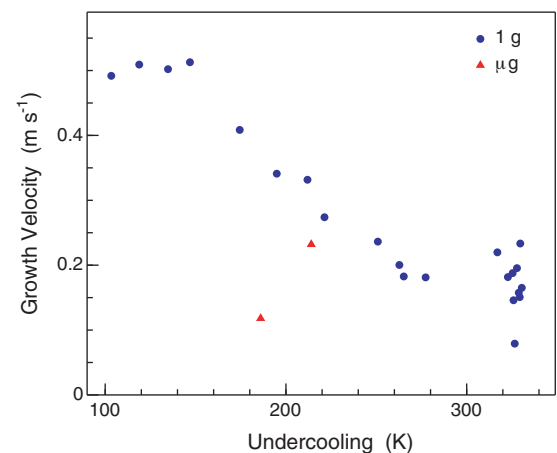


Fig. 4. Dendrite growth velocity V as a function of undercooling, measured for Raney type $\text{Al}_{68.5}\text{Ni}_{31.5}$ alloy on ground (circles) and during TEXUS 44 EML2 flight mission (triangles) [27]. Measurements of growth velocities at undercoolings less than 100 K are not shown. They are normal i.e. the velocity increases with undercooling.

is substantially smaller than the data taken under 1 g conditions. Second, the temperature dependence of the $V(\Delta T)$ relation differs. In reduced gravity, it is apparent that the growth velocity increases with increasing undercooling as being usual for a great variety of alloys. The decrease of the velocity with undercooling as measured on ground on a variety of Al-rich Al–Ni alloys is very anomalous and unique. By taking into account the results of the TEXUS 44 flight this anomalous behaviour of dendrite growth dynamics of Al-rich Al–Ni alloys is obviously associated with gravity dependent mechanism of crystal growth in undercooled melts. A detailed understanding of the experimental results obtained on Earth and in reduced gravity is still lacking up to now.

3.3. Deviations from equilibrium during rapid dendrite growth

During rapid growth of dendrites into deeply undercooled melts several phenomena of deviations from local equilibrium have to be taken into account. In any system, the solid–liquid interface undercools if the velocity of the advancing solidification front becomes comparable to the atomic diffusive speed. In alloys, deviations from chemical equilibrium at the interface have to be considered due to solute trapping. At large undercoolings complete solute trapping leads to the formation of metastable supersaturated solid solutions. In case of intermetallics disorder trapping may occur at high velocities leading to the solidification of disordered superlattice structures [27].

The interface undercooling is controlled by the atomic attachment kinetics. Following rate theory, the transition rates of atoms going from the metastable undercooled state to the solid and vice versa is calculated leading to the well known Wilson–Frenkel equation:

$$V = V_0 \left[1 - \exp\left(-\frac{\Delta G_{LS}}{k_B T}\right) \right] \quad (1)$$

where ΔG_{LS} is the difference of Gibb's free enthalpy between metastable liquid and solid state. V_0 is considered as a temperature dependent factor representing the maximum growth velocity at infinite thermodynamic driving force ΔG_{LS} . By linearization of Eq. (1) under the assumption of $\Delta G_{LS} \ll k_B T$ it yields:

$$V = \left(\frac{V_0}{k_B T}\right) \Delta G_{LS} = \mu \Delta T_k \quad (2)$$

where $\Delta T_k = T_E - T_I$ is the kinetic interface undercooling with T_E the equilibrium melting temperature and T_I the temperature of the interface. μ is the kinetic growth coefficient, which is in between two extremes, either limited by atomic diffusion jumps or atomic collisions. Recently, μ is estimated by molecular dynamic simulations giving values being in between the two extremes either diffusion or collision limited growth assuming that the thermally driven velocity of atoms is the limiting process [28].

In alloys, deviations from chemical equilibrium have to be considered. They are described by a velocity dependent partition coefficient $k(V)$, which is given by [29]:

$$k(V) = \begin{cases} \frac{(1 - (V/V_D)^2)[k_E + (1 - k_E)c_0] + V/V_{Di}}{1 - (V/V_D)^2 + V/V_{Di}}; & V < V_D \\ 1; & V \geq V_D \end{cases} \quad (3)$$

where k_E denotes the equilibrium partition coefficient, c_0 the nominal composition of the alloy, V_D the atomic diffusive speed in liquid and V_{Di} the atomic diffusive speed at the interface. Eq. (3) has been confirmed experimentally by rapid solidification experiments [30,31].

Fig. 5 shows the growth velocity of $\text{Al}_{50}\text{Ni}_{50}$ over the entire undercooling range accessible by levitation. Undercoolings up to $\Delta T \approx 300$ K were measured. For $\Delta T < 240$ K dendrite growth is sluggish. In this regime a superlattice structure of an intermetallic B2

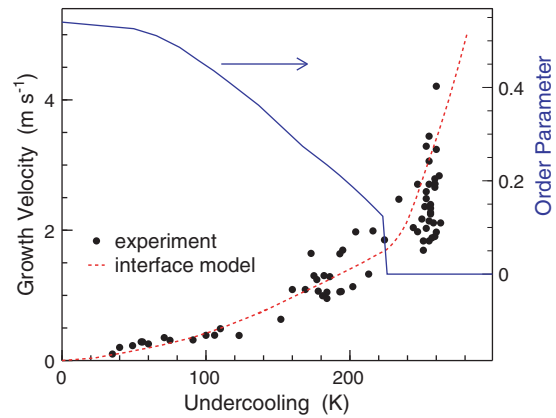


Fig. 5. Dendrite growth velocity, measured for an $\text{Al}_{50}\text{Ni}_{50}$ alloy melt as a function of undercooling. Full circles represent the measured data and the red dashed line gives the data from modelling of dendrite growth. A sharp increase of V sets in at an undercooling of $\Delta T \approx 240$ K at which the order parameter drops down to zero (solid line) [8].

β -phase is formed. Growth is limited by short-range diffusion. The atomic species have to sort them out to find the correct places at the structure of the superlattice. If the undercooling exceeds 240 K the growth velocity rapidly rises with increasing undercooling. This transition is due to a change of crystallization of the ordered β -phase to a disordered superlattice structure. This structural change at the critical undercooling has been unambiguously proven by in situ energy dispersive X-ray diffraction on levitated undercooled $\text{Al}_{50}\text{Ni}_{50}$ samples using a high intensity X-ray beam at the European Synchrotron Radiation Facility in Grenoble [32].

The total undercooling ΔT measured by the experiments consists of several contributions: the thermal undercooling, ΔT_T , the curvature undercooling ΔT_R due to the Gibbs Thomson effect, the constitutional undercooling ΔT_C neglected for congruently melting $\text{Al}_{50}\text{Ni}_{50}$ alloy, and the kinetic interface undercooling ΔT_k . ΔT_R is usually small in particular for thermal dendrites. While at small undercoolings ΔT_T dominates, at large undercoolings ΔT_k progressively becomes more important. Because the solidification of the congruently melting intermetallic phase of $\text{Ni}_{50}\text{Al}_{50}$ requires no long-range diffusion, we assume the validity of the model of collision limited growth for the atomic attachment kinetics of atoms from the liquid to the solid so that the kinetic prefactor V_0 is approximated by the velocity of sound V_S . For sorting of the atoms on the different sublattices, however, diffusion within the solid–liquid interface is required, which is governed by the speed of interface diffusion V_{Di} and by diffusion in the bulk liquid, V_D , which are two to three orders of magnitude smaller than V_S . The balance of the mass fluxes to the different sublattices of the more or less ordered solid phase during crystal growth defines two other kinetic equations [33]. Apart from thermodynamic and kinetic parameters, the equation system depends on five variables. These are the temperature of the solid–liquid interface T_I , the composition of the solid, c_s , and of the liquid phase, c_l , the order parameter η and the growth velocity V . For a given V and at a fixed c_l the other three variables, c_s , T_I and η can be determined by (numerical) solving of the equation system. Hence the model provides a description for the velocity dependence of the order parameter $\eta(V)$.

The results of the computations of dendrite growth velocity as a function of undercooling are given in Fig. 5 (dotted line). It is evident that the predictions of the extended sharp interface model are in reasonable agreement with the experimental results over the entire range of undercooling accessible by application of the electromagnetic levitation technique. At large undercoolings the model reproduces the sharp increase of V at ΔT^* . The solid line in Fig. 5 represents the variation of the order parameter η with undercooling.

It continuously decreases with increasing undercooling and drops suddenly to zero at an undercooling at which disorder trapping sets in as indicated by the sharp increase of dendrite growth velocity. More details are given elsewhere [34,35].

4. Conclusions

Containerless processing by electromagnetic and electrostatic levitation has been applied to investigate crystal nucleation and rapid dendrite growth in undercooled melts of pure zirconium and Al–Ni alloys. Very large undercoolings were achieved. A statistical analysis of the distribution function of maximum undercoolings in electrostatic levitation experiments hints on the onset of homogeneous nucleation. From the homogeneous nucleation rate calculated within classical nucleation theory a lower limit of the solid–liquid interfacial energy was deduced. This value indicates that results by density functional theory and molecular dynamics simulations may lead to an underestimation of the solid–liquid interfacial energies [36]. Comparative experiments on Earth and in reduced gravity of measurements of dendrite growth in undercooled Al₅₀Ni₅₀ clearly reveal the importance of forced convection on growth dynamics which has to be taken into account to predict growth dynamics in undercooled melts in particular in the low undercooling range, in which the dendrite growth velocity is comparable or even less than the fluid flow velocity in electromagnetically levitated melts. An unusual behaviour of growth dynamics in Al_{68.5}Ni_{31.5} alloy was found such that the growth velocity decreases with increasing undercooling. Comparative measurements in reduced gravity hint on a possible influence of forced convection to be the origin of this unusual growth behaviour. Finally, non-equilibrium effects during rapid dendrite growth were discussed, comprising an interface undercooling due to the limited atomic attachment kinetics and solute trapping during rapid solidification of alloys. By measurements of the dendrite growth velocity of the equiatomic Al–Ni alloy at very large undercoolings a transition from ordered to disordered growth of the B2 β-phase was identified. By taking into account a velocity dependent order parameter dendrite growth theory was extended such that it describes quantitatively the dendrite growth velocity over the entire undercooling range accessible by containerless processing.

Acknowledgements

The author thanks Peter Galenko, Helena Hartmann, Dirk Holland-Moritz, Stefan Klein, Roman Lengsdorf for useful discussions. Financial support by Deutsche Forschungsgemeinschaft within contracts HE1601/18 and HE1601/22, DLR Space Agency

within contract 50WM0736, and the European Space Agency within contract 15236/02/NL/SH is gratefully acknowledged.

References

- [1] W. Ostwald, *Zeitschrift für Physikalische Chemie* 22 (1897) 289.
- [2] J.W. Christian, *The Theory of Transformation in Metals and Alloys*, Pergamon, Oxford, 1975.
- [3] D.M. Herlach, *Annual Review of Materials Science* 21 (1991) 23.
- [4] T. Meister, H. Werner, G. Lohöfer, D.M. Herlach, H. Unbehauen, *Engineering Practice* 11 (2003) 117.
- [5] J.A. Dantzig, M. Rappaz, *Solidification*, EPFL Press, Lausanne, 2010 (Chapter 8).
- [6] R.W. Hyers, *Measurement Science and Technology* 16 (2005) 394.
- [7] C.B. Arnold, M.J. Aziz, M. Schwarz, D.M. Herlach, *Physical Review B* 59 (1999) 334.
- [8] H. Hartmann, D. Holland-Moritz, P. Galenko, D.M. Herlach, *Europhysics Letters* 87 (2009) 40007.
- [9] O. Funke, G. Phanikumar, P.K. Galenko, L. Chernova, S. Reutzel, M. Kolbe, D.M. Herlach, *Journal of Crystal Growth* 297 (2006) 211.
- [10] J. Piller, R. Knauf, P. Preu, D.M. Herlach, G. Lohöfer, *Proceedings 6th European Symposium on Materials Sciences under Microgravity ESA SP-256, Bordeaux, 1986*, p. p437.
- [11] A. Rulison, W. Rhim, *Review of Scientific Instruments* 65 (1993) 695.
- [12] G. Wilde, G.P. Görler, R. Willnecker, *Applied Physics Letters* 69 (1996) 2953; G. Wilde, G.P. Görler, R. Willnecker, *Applied Physics Letters* 68 (1996) 2955.
- [13] V. Skripov, *Material Science, Crystal Growth and Materials* (1977).
- [14] W. Hofmeister, C. Morton, R. Bayuzick, *Acta Materialia* 46 (1998) 1903.
- [15] T. Schenk, D. Holland-Moritz, D. Herlach, *Europhysics Letters* 50 (2000) 402.
- [16] S. Klein, D. Holland-Moritz, D.M. Herlach, *Physical Review B* 80 (2009) 212202.
- [17] D.R. Nelson, F. Spaepen, *Solid State Physics*, Academic, New York, 1989.
- [18] D.W. Marr, A.P. Gast, *Journal of Chemical Physics* 99 (1993) 2024.
- [19] D.Y. Sun, M. Asta, J.J. Hoyt, *Physical Review B* 69 (2004) 174103.
- [20] T. Schenk, D. Holland-Moritz, V. Simonet, R. Bellissent, D.M. Herlach, *Physical Review Letters* 89 (2002) 075507.
- [21] G.W. Lee, A.K. Gangopadhyay, K.F. Kelton, R.W. Hyers, T.J. Rathz, J.R. Rogers, D.S. Robinson, *Physical Review Letters* 93 (2004) 037802.
- [22] S. Reutzel, H. Hartmann, P.K. Galenko, S. Schneider, D.M. Herlach, *Applied Physics Letters* 91 (2007) 041913.
- [23] M. Barth, B. Wei, D.M. Herlach, *Physical Review B* 51 (1995) 3422.
- [24] D.M. Herlach, P.K. Galenko, *Materials Science and Engineering A* 449–451 (2007) 34.
- [25] O. Shuleshova, D. Holland-Moritz, W. Löser, G. Reinhart, G. Iles, B. Büchner, *Europhysics Letters* 86 (2009) 36002.
- [26] R. Lengsdorf, D. Holland-Moritz, D.M. Herlach, *Scripta Materialia* 62 (2010) 365.
- [27] For more details, see e.g.: D.M. Herlach, P. K. Galenko, D. Holland-Moritz, in: Robert Cahn (Ed.), *Metastable Materials from Undercooled Melts*, Pergamon Materials Series, 2007.
- [28] J.J. Hoyt, M. Asta, T. Haxhimali, A. Karma, R.E. Napolitano, R. Trivedi, B.B. Laird, J.R. Morris, *MRS Bulletin* 29 (2004) 935.
- [29] P.K. Galenko, S.L. Sobolev, *Physical Review E* 55 (1997) 343.
- [30] J.A. Kittl, P.G. Sanders, M.J. Aziz, D.P. Brunco, M.O. Thomson, *Acta Materialia* 48 (2000) 4797.
- [31] C. Arnold, M.J. Aziz, M. Schwarz, D.M. Herlach, *Physical Review B* 59 (1999) 334.
- [32] H. Hartmann, D. Holland-Moritz, P.K. Galenko, D.M. Herlach, *Europhys. Lett.* 87 (2009) 40007.
- [33] H. Assadi, S. Reutzel, D.M. Herlach, *Acta Materialia* 54 (2006) 2793.
- [34] H. Hartmann, PhD Thesis Ruhr-Universität Bochum, 2008.
- [35] This is subject of a forthcoming paper, presently in progress.
- [36] S. Klein, D. Holland-Moritz, D.M. Herlach, *Physical Review B* 80 (2009) 212202 (BR).